Supplement of

Modelling Glacier Evolution in Bhutanese Himalaya during the Little Ice Age

Weilin Yang[1], Yingkui Li[2], Gengnian. Liu[1], Wenchao Chu[3]

[1]College of Urban and Environmental Sciences, Peking University, Beijing 100871, China.
[2]Department of Geography, University of Tennessee, Knoxville, TN 37996, USA.
[3]Department of Earth System Science, Ministry of Education Key Laboratory for Earth System Modeling, Institute for Global Change Studies, Tsinghua University, Beijing 100084, China.

Correspondence to: Wenchao Chu (peterchuwenchao@foxmail.com)

Contents of this file:

Text S1. Moraine age determination

We chose 126 ^{10}Be surface exposure dating ages across the monsoon-influenced Himalaya for regional LIA chronological comparison and applied the following criteria to ensure valid comparisons. The results are shown in Table S1.

(1) All published ^{10}Be ages are recalculated using CRONUS Earth V3 online calculator (Balco et al., 2008; http://hess.ess.washington.edu/math/). In the interpretation, we focus on the ages calculated using the time and nuclide-dependent scaling scheme 'LSDn' (Lifton, et al., 2014).

(2) A set of ^{10}Be ages from the same moraine are usually scattered due to nuclide inheritance, such as prior exposure and incomplete exposure caused by geographic shielding or post weathering processes (Heyman et al., 2011). Therefore, statistical treatment is of importance to identify potential outliers and to determine the depositional ages of any moraines (Owen & Dortch, 2014). We applied the Peirce's criterion to detect outliers (Peirce, 1852; Ross, 2003). Peirce's criterion is a rigorous method based on probability theory. An exposure age can be considered as an outlier if the deviation from the group mean is larger than the maximum allowed deviation. The threshold is determined by multiplying the standard deviation of all samples and the *R* (the ratio of the maximum allowable value from the data mean to the standard deviation), using Peirce's criterion table (Peirce, 1852; Ross, 2003; Peng et al., 2019). The internal uncertainties of all ^{10}Be ages are used in Peirce's criterion. However, it will not identify any outlier if a group of samples are evenly spread out, even if it is obvious that the ages do not overlap (Yang et al., 2021). Thus, we removed the outliers for these ^{10}Be ages according the original published articles and the moraine relative geomorphological positions, morphology and weathering conditions.

(3) After removing outlier(s), the reduced χ^2 statistic (χ^2_R) was calculated to test if any remaining ages were scattered (Balco, 2011). If the χ^2_R is insignificant at the 95% confidence level (p>0.05), the scatter can be explained by measurement errors, so the weighted mean was used for moraine age interpretation; if χ^2_R is statistically significant (P>0.05), the scatter is likely caused by prior inheritance or incomplete exposure, thus a range of plausible ages is summarized for the moraine (Chen et al., 2015; Li et al., 2016).

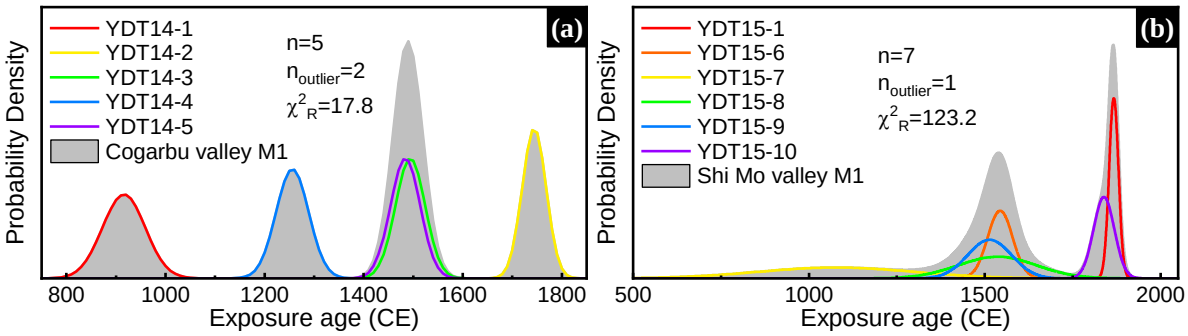

Figure S1. Probability density plots of ^{10}Be surface exposure ages with internal uncertainty for moraines (a) Cogarbu valley M1 and (b) Shi Mo valley M1 in BH, and the reduced χ^2 statistic (χ^2_R) after removing outliers. The Gauss distribution of each age is plotted with the mean and standard deviation. The cumulative probability density function (PDF; grey shaded area) is created by summing probability densities of all ages. These PDFs illustrate the cluster of the ages and potential outliers.

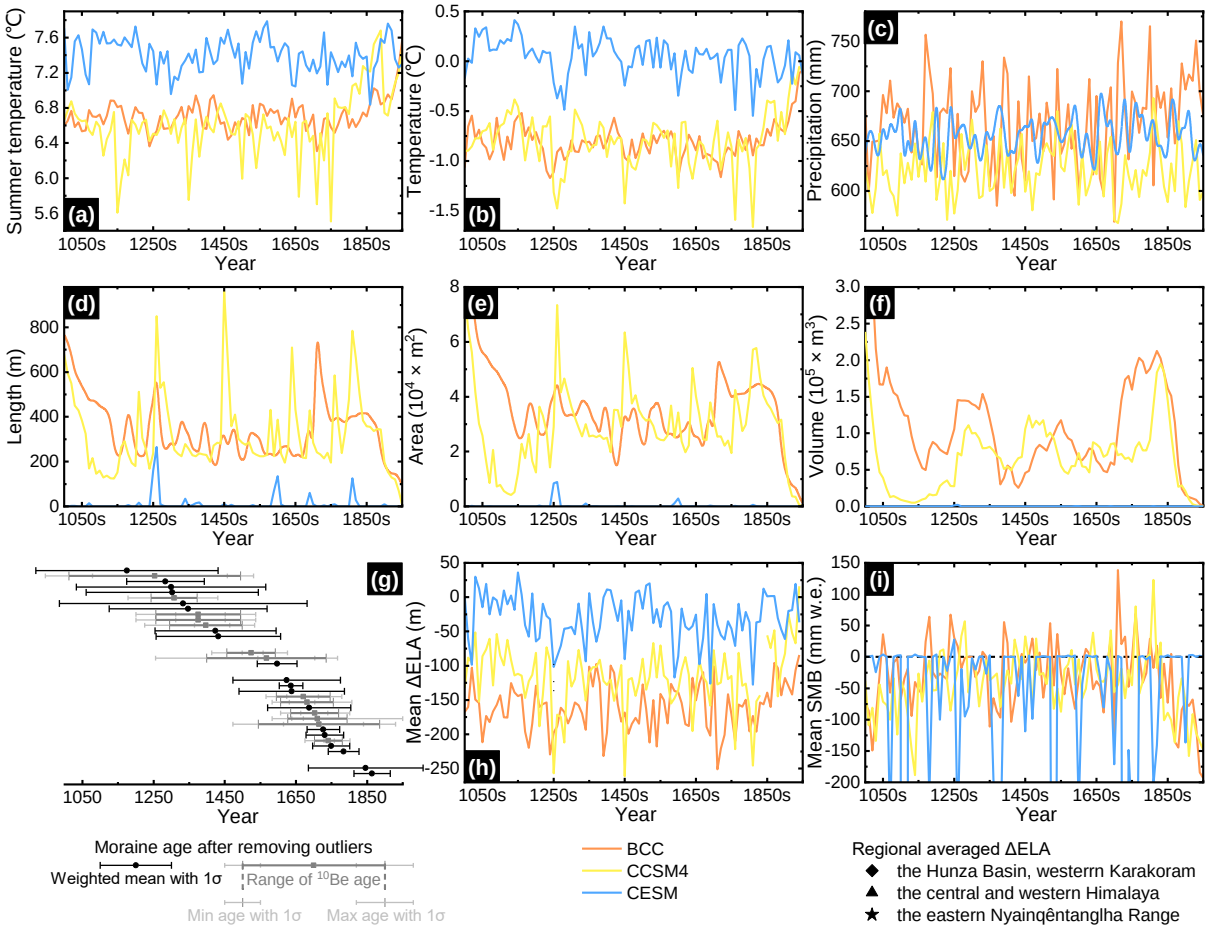

Figure S2. Interannual (a) summer temperature, (b) temperature, and (c) precipitation changes from 1000s to 1950s averaged over Bhutanese Himalaya. Glacier (d) length, (e) area, (f) volume, (h) ELA, and (i) SMB changes during LIA across the studied area,

modelled by OGGM using three separate GCM produces (BCC, CCSM4, and CESM). Each glacier in the OGGM runs has its length, area, volume, and ELA changes normalized relative to the corresponding averaged parameters during 1950s in the run output. Besides, the recalculated moraine ages across the monsoon-influenced Himalaya are also shown (g). The regional averaged ΔELAs are illustrated in Figure 2h.

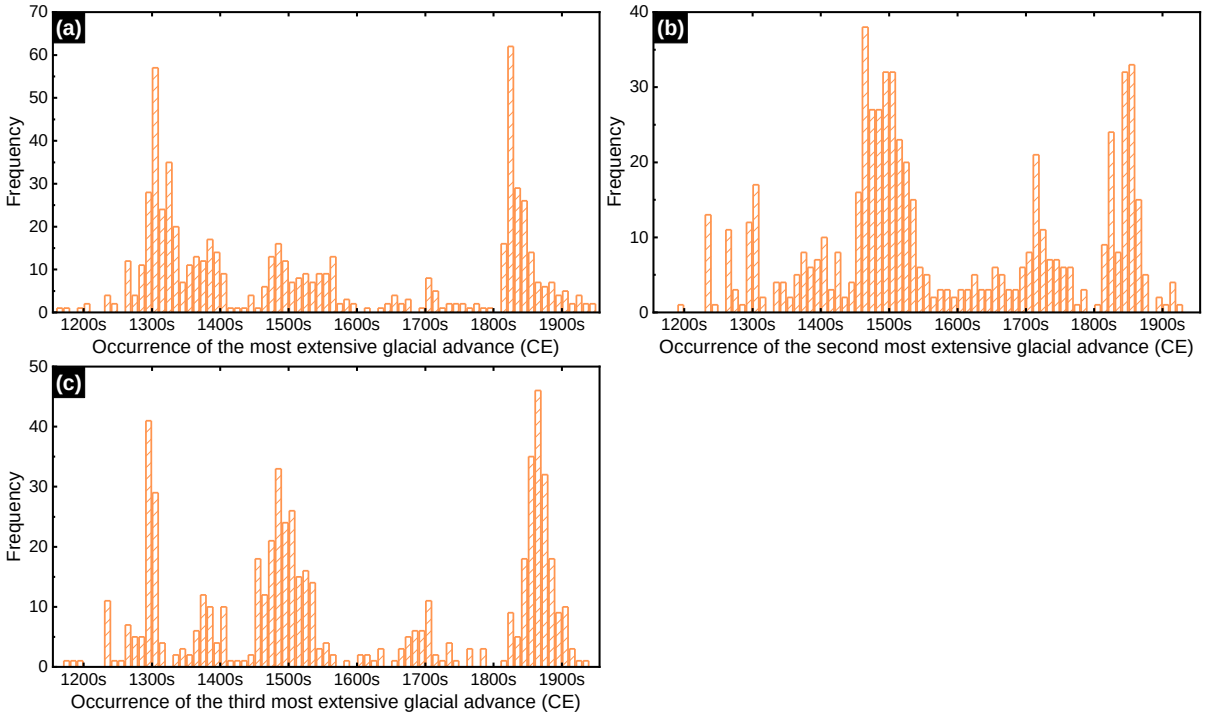

Figure S3. The frequency distribution chart shows the occurrence of the most (a), second most (b), and third most (c) extensive glacial advance of each glacier for the GISS experiment.

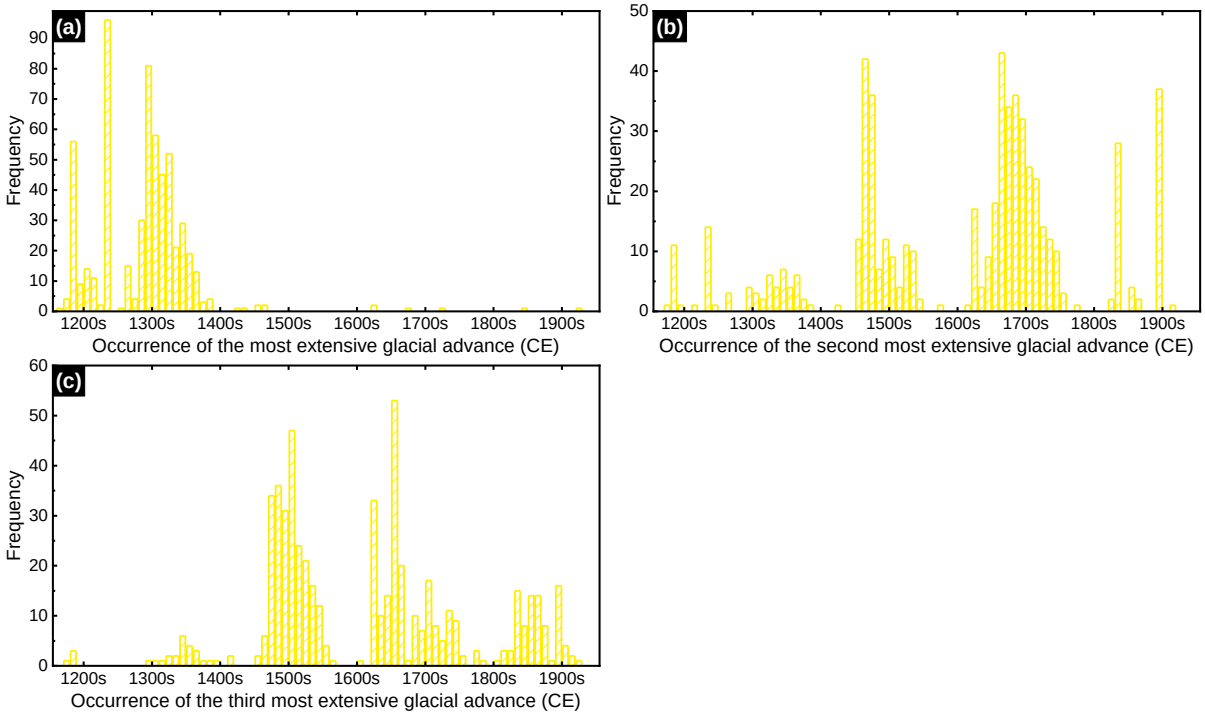

Figure S4. The frequency distribution chart shows the occurrence of the most (a), second most (b), and third most (c) extensive glacial advance of each glacier for the IPSL experiment.

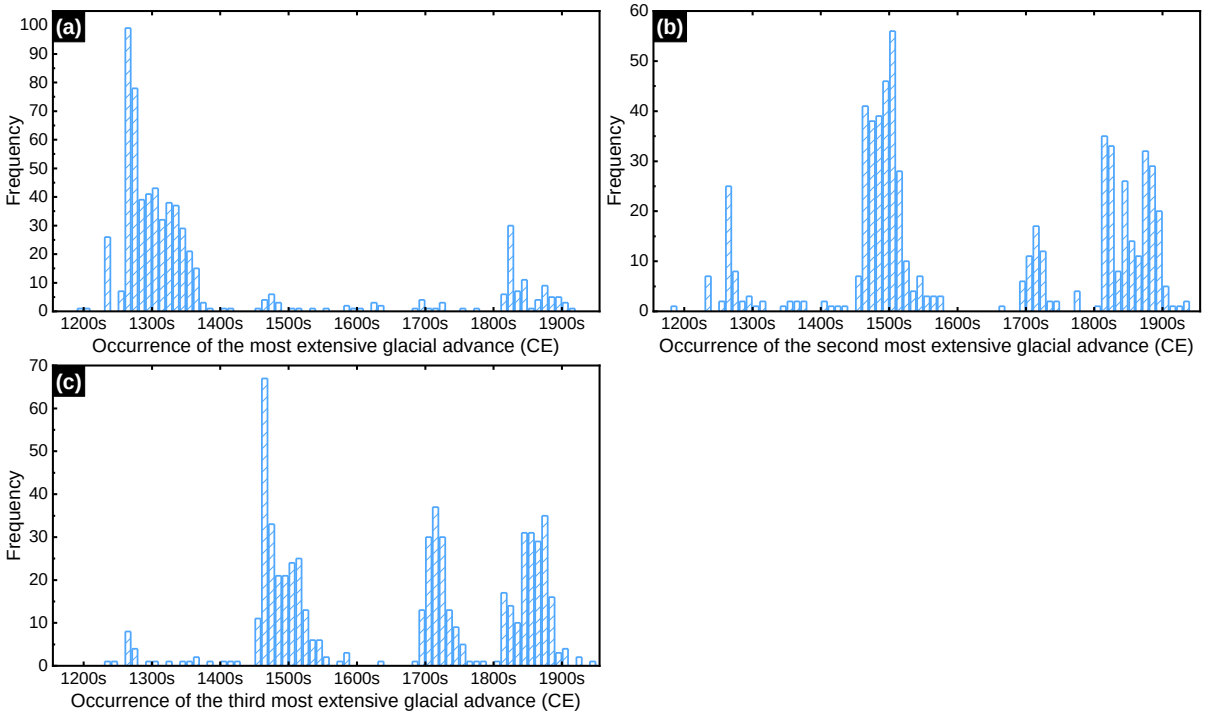

Figure S5. The frequency distribution chart shows the occurrence of the most (a), second most (b), and third most (c) extensive glacial advance of each glacier for the MPI experiment.

Table S1. Recalculated previously published minimum ^{10}Be surface exposure ages in the monsoon-influenced Hiamlaya using the CRONUS Earth V3 online calculator with the time-dependent scaling scheme "LSDn".

Location and Source	Moraine	Sample ID	Latitude (°)	Longitude (°)	Elevation (m)	Thickness (cm)	Topographic shielding factor	^{10}Be Concentration (atoms/g)	Recalculated ^{10}Be age (ka)	Moraine age (CE)
Bhutanese Himalaya; Peng et al. (2019)	M1, Cogarbu valley	YDT14-1[(1)]	28.2386	89.8913	4955	5	0.9735	58500 ± 2300	1098 ± 78	1256 ± 56 - 1494 ± 43
		YDT14-2[(1)]	28.2383	89.8915	4946	5	0.9743	12300 ± 1100	270 ± 29	
		YDT14-3	28.239	89.8911	4947	5	0.9735	24200 ± 1400	520 ± 43	
		YDT14-4	28.2397	89.8906	4945	4	0.9657	36300 ± 1600	758 ± 56	
		YDT14-5	28.2401	89.8904	4942	5	0.9657	24500 ± 1400	530 ± 44	
Bhutanese Himalaya; Peng et al. (2020)	M1, Shimo valley	YDT15-1	28.2851	89.99504	5064	3	0.99	7387 ± 607	147 ± 15	1077 ± 228 - 1867 ± 15
		YDT15-4[(1)]	28.2852	89.9949	5072	3	0.99	144194 ± 3240	2614 ± 165	
		YDT15-6	28.2838	89.9938	5103	4	0.92	22257 ± 1646	470 ± 44	
		YDT15-7	28.2837	89.99367	5104	5	0.92	47302 ± 11166	937 ± 228	
		YDT15-8	28.2837	89.99375	5103	5	0.92	22466 ± 5240	478 ± 115	
		YDT15-9	28.2837	89.99385	5100	5	0.97	24796 ± 3072	500 ± 69	
		YDT15-10	28.2833	89.99351	5107	4	0.98	8768 ± 1443	175 ± 31	
Lahul Himalaya; Saha et al. (2018)	$m_{H1a,}$ Hamtah valley	HAMTAH-1405	32.2725	77.35738	4014	2	0.9429	8900 ± 1900	281 ± 62	1200 ± 93 - 1837 ± 32
		HAMTAH-1406	32.2722	77.3575	4023	1	0.9444	15600 ± 4100	463 ± 125	
		HAMTAH-1408[(1)]	32.2686	77.35847	4111	2.5	0.9540	90600 ± 5500	2209 ± 187	
		HAMTAH-1410	32.2678	77.35892	4125	2.5	0.9476	6000 ± 1000	179 ± 32	
		HAMTAH-1502	32.2954	77.36555	3861.182	2	0.9233	25700 ± 2500	816 ± 93	
	m_{A1}, Lato valley	LATO-1415[(2)]	33.6822	77.59202	5366	3	0.9501	133100 ± 3100	1603 ± 102	1595 ± 29 - 1746 ± 33
		LATO-1416	33.6822	77.5921	5358	4	0.9501	16600 ± 1800	270 ± 33	
		LATO-1417	33.6826	77.59203	5348	2	0.9508	27400 ± 1000	421 ± 29	
		LATO-1418	33.6826	77.59207	5351	3	0.9459	17900 ± 1400	290 ± 28	
		LATO-1419[(2)]	33.6827	77.592	5339	3	0.9517	246600 ± 18500	3162 ± 302	
	m_{A2c}, Lato valley	LATO-1409[(2)]	33.6851	77.59525	5314	3	0.9593	2651000 ± 56400	26351 ± 1664	1456 ± 43 - 1592 ± 34
		LATO-1410[(2)]	33.6851	77.59531	5321	2.5	0.9593	218600 ± 8700	2862 ± 204	
		LATO-1411[(2)]	33.6851	77.5952	5315	2	0.9593	296300 ± 17800	3861 ± 325	
		LATO-1412	33.685	77.59566	5315	1	0.9576	27600 ± 1500	424 ± 34	
		LATO-1413[(1)]	33.6849	77.59573	5317	2	0.9594	57700 ± 2000	828 ± 57	
		LATO-1414	33.6851	77.59538	5314	2	0.9596	37600 ± 1800	560 ± 43	
	m_{M1}, Karzok valley	KO-7[(1)]	32.933	78.214	5524	6	1	20400 ± 1400	306 ± 28	1283 ± 109
		KO-8	32.933	78.214	5516	2.5	1	59200 ± 5500	782 ± 86	
		KO-9	32.934	78.215	5503	1	1	60000 ± 2400	786 ± 56	
		KO10	32.934	78.215	5503	1	1	47300 ± 6700	630 ± 97	

Annapurna; Zech et al. (2009)	Dudh Khola Valley	DK11	28.627	84.467	3650	2	0.942	3950 ± 3910	162 ± 161	1846 ± 161
Lhagoi Kangri Range; Liu et al. (2017)	M1A, Karola Pass	TB-14-33	28.9502	90.1346	4988	3	0.937	6960 ± 3350	150 ± 73	1864 ± 51
		TB-14-34	28.9498	90.1344	4996	5	0.94	6760 ± 810	147 ± 20	
		TB-14-36(1)	28.9492	90.1342	5012	3	0.936	12390 ± 680	267 ± 22	
	M1B, Karola Pass	TB-14-39	28.9493	90.1338	5017	6	0.944	14270 ± 870	312 ± 27	1702 ± 27 - 1780 ± 22
		TB-14-41	28.9508	90.134	4980	3	0.952	10900 ± 800	234 ± 22	
		TB-14-42(1)	28.9506	90.134	4980	6	0.958	19250 ± 4540	416 ± 101	
Nepal Himalaya; Barnard et al. (2006)	inner moraine, Langtang Khola Valley	KTM4	28.21	85.56	3924	5	0.97	25000 ± 8000	741 ± 241	1302 ± 242
		KTM5(1)	28.21	85.56	3922	5	0.97	44000 ± 12000	1166 ± 325	
		KTM6	28.21	85.56	3923	5	0.97	22000 ± 8000	658 ± 242	
	outer moraine, Langtang Khola Valley	KTM7	28.21	85.57	3840	5	0.98	27000 ± 9000	817 ± 277	1175 ± 256
		KTM8	28.21	85.57	3838	5	0.98	28000 ± 8000	845 ± 246	
		KTM9(1)	28.21	85.57	3839	5	0.98	33000 ± 10000	965 ± 298	
Garhwal; Murari et al. (2014)	m_{bd4}, Bhillangana and Dudhganga valleys	KAL7	30.7898	78.9522	3635	3	0.911	6800 ± 1200	282 ± 53	1731 ± 53
		KAL9(1)	30.7897	78.9523	3637	3	0.911	1700 ± 300	69 ± 13	
	m_{bd3}, Bhillangana and Dudhganga valleys	KAL10	30.7839	78.9511	3579	3	0.937	6200 ± 1200	258 ± 52	1607 ± 24 - 1755 ± 52
		KAL11	30.7838	78.9509	3576	2.5	0.937	7000 ± 900	291 ± 41	
		KAL12(2)	30.7836	78.9507	3568	2	0.937	47300 ± 2500	1596 ± 126	
		KAL13(2)	30.7834	78.9504	3571	3	0.943	69300 ± 3200	2510 ± 188	
		KAL14	30.7831	78.9501	3571	2.5	0.938	10000 ± 100	406 ± 24	
	m_{bd2}, Bhillangana and Dudhganga valleys	KAL1	30.7778	78.9515	3641	1.5	0.937	9900 ± 800	386 ± 39	1597 ± 56
		KAL2	30.7777	78.9512	3650	2	0.923	11400 ± 1200	445 ± 54	
		KAL3(2)	30.7782	78.9506	3646	1.5	0.935	2500 ± 300	98 ± 13	
		KAL4(2)	30.7782	78.9504	3657	1.5	0.923	500 ± 200	19 ± 8	
		KAL5(2)	30.7782	78.9533	3644	5	0.929	2300 ± 300	94 ± 13	
	m_{bd1}, Bhillangana and Dudhganga valleys	KAL18	30.7565	78.9629	4132	2	0.949	8600 ± 1200	263 ± 40	1727 ± 46
		KAL19	30.7585	78.9627	4182	2	0.937	10700 ± 800	322 ± 31	
		KAL20(2)	30.7567	78.9628	4115	2	0.94	36400 ± 3000	999 ± 101	
		KAL21	30.7567	78.9653	4108	2	0.939	8700 ± 1200	272 ± 41	
	m_{k2}, Kedarnath	KAL35	30.7448	79.6503	3841	4	0.953	18100 ± 4100	614 ± 144	1399 ± 144 - 1735 ± 32
		KAL36	30.7454	79.0652	3853	5	0.95	8000 ± 900	289 ± 37	
		KAL37	30.7462	79.0655	3884	3	0.959	722000 ± 222000	17750 ± 5582	
		KAL38	30.7473	79.0661	3909	5	0.959	8000 ± 800	278 ± 32	
		KAL39(2)	30.7478	79.0662	3915	2.5	0.096	12200 ± 2200	3286 ± 624	
central Gangdise Mountains; Zhang et al. (2018a)	M2, Lopu Kangri Area	13GDS5-1	29.8182	84.6951	5499	2.3	0.9987	16841 ± 5336	272 ± 88	1749 ± 52
		13GDS5-2	29.8183	84.69497	5502	2.3	0.9987	15443 ± 1656	249 ± 30	
		13GDS5-3	29.8184	84.69493	5499	1.6	0.9987	15852 ± 1738	254 ± 32	
		13GDS5-4	29.8184	84.69494	5499	2.3	0.9987	16802 ± 2471	271 ± 43	
		13GDS5-5	29.8184	84.69492	5499	2.1	0.9987	17103 ± 2123	276 ± 38	
		14GDS1-1(1)	29.8199	84.69476	5487	2.7	0.9991	24815 ± 1263	396 ± 31	1636 ± 33

	M3, Lopu Kangri Area	14GDS1-2	29.8197	84.69494	5487	1.8	0.9991	24372 ± 1496	387 ± 33	
		14GDS1-3[(1)]	29.8197	84.69493	5490	2.1	0.9991	22040 ± 1462	353 ± 31	
		14GDS1-4	29.8197	84.69496	5489	2.3	0.9991	23087 ± 1329	369 ± 30	
	M4, Lopu Kangri Area	13GDS6-1	29.8185	84.69688	5497	2.2	0.9992	17083 ± 5786	276 ± 95	1638 ± 148
		13GDS6-2	29.8185	84.69686	5495	2.3	0.9992	29569 ± 9646	464 ± 154	
		13GDS6-3[(1)]	29.8185	84.69686	5495	2	0.9992	83279 ± 11788	1109 ± 170	
		13GDS6-4	29.8186	84.6968	5495	2	0.9992	24311 ± 7756	386 ± 125	
	M5, Lopu Kangri Area	13GDS7-1	29.8191	84.69875	5507	1.9	0.9995	24986 ± 6518	393 ± 105	1687 ± 117
		13GDS7-2	29.8195	84.69881	5504	2.1	0.9996	15735 ± 7287	253 ± 118	
		13GDS7-3	29.8195	84.69893	5507	1.6	0.9996	18660 ± 7520	298 ± 121	
		13GDS7-4	29.8195	84.69896	5508	2	0.9996	22186 ± 5085	352 ± 83	
		13GDS7-5[(1)]	29.8196	84.69889	5508	2	0.9996	44702 ± 9611	677 ± 151	
Himalaya; Owen et al. (2009)	T7, Mount Everest	Ron-51	28.13	86.853	5216	4	0.97	11000 ± 8000	214 ± 156	1627 ± 44 - 1794 ± 156
		Ron-53	28.129	86.854	5213	2	0.97	20000 ± 2000	381 ± 44	
		Ron-55[(1)]	28.13	86.856	5225	2	0.97	39000 ± 3000	716 ± 69	
Gurla Mandhata; Owen et al. (2010)	M10, Muguru Valley	Na48	30.463	81.217	5508	2	0.946	29000 ± 4100	465 ± 71	1544 ± 71 - 1885 ± 45
		Na49[(2)]	30.463	81.217	5506	1	0.946	229900 ± 6500	3178 ± 208	
		Na50	30.463	81.217	5509	2	0.946	7500 ± 2700	124 ± 45	
		Na52[(2)]	30.464	81.217	5514	2	0.952	280900 ± 6900	3932 ± 252	
		Na53	30.464	81.216	5509	2	0.955	17800 ± 1200	294 ± 26	
West Himalaya; Dortch et al. (2013)	Pangong Cirque, Ladakh, Nn India	Pang-24[(1)]	33.888	78.425	5375	5	1	14824 ± 6621	229 ± 103	1347 ± 222
		Pang-25[(1)]	33.888	78.425	5375	5	1	162492 ± 37623	1885 ± 451	
		Pang-26	33.888	78.425	5368	5	1	49909 ± 8581	698 ± 127	
		Pang-27	33.888	78.425	5371	5	1	57723 ± 19329	793 ± 270	
		Pang-28[(1)]	33.888	78.426	5363	5	1	163049 ± 23407	1902 ± 295	
		Pang-29	33.888	78.426	5360	4	1	35547 ± 9858	509 ± 144	
Northwestern India; Lee et al. (2014)	TG3, Nun-Kun massif	NK29	34.06	75.92	3679	2.5	0.96	15631 ± 513.7	513 ± 35	1295 ± 70 - 1499 ± 35
		NK-30	34.05	75.92	3720	4	0.96	22600 ± 1764.7	717 ± 70	
Garhwal; Scherler et al. (2010)	Jaundhar Glacier, Tons Valley	DS6-057	31.142	78.454	3636	3	0.95	13695 ± 538	515 ± 37	1012 ± 66 - 1494 ± 37
		DS6-058	31.142	78.453	3623	3	0.94	28171 ± 821	997 ± 66	
	Bandarpunch Glacier	DS6-032	31.072	78.499	4071	3	0.95	12086 ± 551	374 ± 28	1635 ± 28 - 1770 ± 31
		DS6-033	31.072	78.498	4046	2	0.97	7688 ± 873	239 ± 31	
Garhwal Himalaya; Barnard et al. (2004a)	m4, Gori Ganga Valley	NDL2	30.45	80.12	3534	5	0.97	14000 ± 5000	492 ± 178	1299 ± 266
		NDL4	30.45	80.12	3522	5	0.96	27000 ± 4000	915 ± 146	
	M3, Gori Ganga Valley	NDL9	30.45	80.13	3505	5	0.97	7000 ± 5000	261 ± 187	1624 ± 151
		NDL10	30.45	80.13	3510	5	0.98	13000 ± 2000	461 ± 76	
Garhwal Himalaya; Barnard et al. (2004b)	Gangotri glacial stage, Upper Bhagirathi Valley	BH29	30.945	79.061	3973	5	0.97	31241 ± 8369	821 ± 225	1333 ± 348
		BH30	30.945	79.062	3956	5	0.97	15261 ± 6683	427 ± 189	
		BH31	30.945	79.062	3973	5	0.97	11177 ± 6842	319 ± 196	
		BH32	30.945	79.062	3956	5	0.97	43712 ± 7013	1065 ± 182	
Annapurna Range;	E moraine crest,	NP222[(1)]	28.635	84.042	4000	2	0.91	43480 ± 6510	1141 ± 184	1424 ± 170
		NP223	28.635	84.042	3813	2	0.912	23060 ± 3620	743 ± 125	

Heimsath & McGlynn (2008)	Milarepa's Glacier	NP233	28.635	84.042	4275	2	0.907	15090 ± 3380	401 ± 93	
		NP234	28.635	84.042	4216	2	1	24830 ± 1990	601 ± 60	
		NP235(1)	28.635	84.042	4157	2	0.91	43480 ± 6510	210 ± 22	
	W moraine crest, Milarepa's Glacier	NP212	28.641	84.044	3844	2	1	26460 ± 1620	763 ± 65	1243 ± 65 - 1372 ± 58
		NP213(1)	28.641	84.044	3797	2	0.935	7042 ± 1780	234 ± 61	
		NP214	28.641	84.044	3669	2	1	19810 ± 1400	634 ± 58	
Nun Kun massif; Saha et al. (2019)	M_{P1}, Parkachik valley	PAR1601	34.0835	75.9998	3700	2	0.968	5600 ± 600	192 ± 23	1784 ± 43
		PAR1602(1)	34.0844	76.0001	3687	3	0.973	3300 ± 800	114 ± 28	
		PAR1603	34.0846	76.0002	3678	3.5	0.974	7100 ± 500	247 ± 23	
		PAR1606	34.085	76.0004	3667	2	0.969	7400 ± 1200	257 ± 44	
Lahul massif; Saha et al. (2019)	M_{k2}, Kulti valley	S9	32.4233	77.3067	3676	2	0.917	12700 ± 4600	468 ± 172	1432 ± 175
		S10	32.4233	77.3067	3678	2	0.913	19500 ± 1900	699 ± 80	

Notes: (1) mean the potential outlier defined by Peirce's criterion;

(2) mean the potential outlier removed according to original published.

Table S2. Climate model simulations used to drive OGGM.

Name	Institution	Resolution (lat × lon)	Reference	Time (CE)
CCSM4	National Center for Atmospheric Research	192 × 288	Gent et al. (2011)	850-2006
CESM1	National Center for Atmospheric Research	96 × 144	Otto-Bliesner et al. (2016)	850-2005
GISS-E2-R	NASA Goddard Institute for Space Studies	90 × 144	Schmidt et al. (2014)	850-2005
IPSL-CM5A-LR	Institut Pierre-Simon- Laplace	96 × 96	Dufresne et al. (2013)	850-2006
MPI-ESM-P	Max Planck Institute for Meteorology	96 × 192	Stevens et al. (2013)	850-2005
BCC-CSM1-1	Beijing Climate Center, China Meteorological Administration	64 × 128	Wu et al. (2014)	850-2000
CRU TS4.01	Climatic Research Unit gridded Time Series	360 × 720	Harris et al. (2020)	1901-2018

Table S3. Table shows the occurrence of each substage during LIA. Meanwhile, the maximum of the modelled glacier length, area, and volume changes during each substage are also shown in this table. Data is displayed for GISS, IPSL, MPI for all modelled glacier in BH.

Event	LIA-4			LIA-3			LIA-2			LIA-1		
	GISS	IPSL	MPI	GISS	IPSL	MPI	GISS	IPSL	MPI	GISS	IPSL	MPI
Age (CE)	1400s	1330s	1270s	1520s	1520s	1470s	1710s	1700s	1700s	1880s	1900s	1820s
ΔLength (%)	72.9	97.6	117.7	61.4	73.3	76.6	37.9	79.0	61.7	55.6	56.4	70.9

ΔArea (%)	175.0	221.9	106.8	154.9	163.2	100.8	127.8	178.4	96.0	141.5	128.9	109.6
ΔVolume (%)	465.7	589.7	467.0	416.8	412.5	568.4	354.7	435.7	567.5	395.5	342.2	648.8

References

Balco. G.: Contributions and unrealized potential contributions of cosmogenic-nuclide exposure dating to glacier chronology, 1990-2010, *Quaternary. Sci. Rev.*, *30*, 3-27, https://doi.org/10.1016/j.quascirev.2010.11.003, 2011.

Balco, G., Stone, J.O., Lifton, N.A., and Dunai, T.J.: A complete and easily accessible means of calculating surface exposure ages or erosion rates from ^{10}Be and 26Al measurements, *Quat. Geochronol.*, *3*, 174-195, https://doi.org/10.1016/j.quageo.2007.12.001, 2008.

Barnard, P.L., Owen, L.A., & Finkel, R.C.: Style and timing of glacial and paraglacial sedimentation in a monsoon-influenced high Himalayan environment, the upper Bhagirathi Valley, Garhwal Himalaya, *Sediment. Geol.*, *165*, 199-221, https://doi.org/10.1016/j.sedgeo.2003.11.009, 2004a.

Barnard, P.L., Owen, L.A., Finkel, R.C., and Asahi, K.: Landscape response to deglaciation in a high relief, monsoon-influenced alpine environment, Langtang Himal, Nepal, *Quaternary. Sci. Rev.*, *25*, 2162-2176, https://doi.org/10.1016/j.quascirev.2006.02.002, 2006.

Barnard, P.L., Owen, L.A., Sharma, M.C., and Finkel, R.C.: Late Quaternary (Holocene) landscape evolution of a monsoon-influenced high Himalayan valley, Gori Ganga, Nanda Devi, NE Garhwal, *Geomorphology*, *61*, 91-110, https://doi.org/10.1016/j.geomorph.2003.12.002, 2004b.

Chen, Y., Li, Y., Wang, Y., Zhang, M., Cui, Z., Yi, C., and Liu, G.: Late Quaternary glacial history of the Karlik Range, easternmost Tian Shan, derived from ^{10}Be surface exposure and optically stimulated luminescence datings, *Quaternary. Sci. Rev.*, *115*, 17-27, http://dx.doi.org/10.1016/j.quascirev.2015.02.010, 2015.

Dortch, J.M., Owen, L.A., and Caffee, M.W.: Timing and climatic drivers for glaciation across semi-arid western Himalayan-Tibetan orogen, *Quaternary. Sci. Rev.*, *78*, 188-208, http://dx.doi.org/10.1016/j.quascirev.2013.07.025, 2013.

Dufresne, J. L., Foujols, M., Denvil, S., Caubel, A., Marti, O., Aumont, O., Balkanski, Y., Bekki, S., Bellenger, H., Benshila, R., Bony, S., Bopp, L., Braconnot, P., Brockmann, P., Cadule, P., Cheruy, F., Codron, F., Cozic, A., Cugnet, D., de Noblet, N., Duvel, J. P., Ethé, C., Fairhead, L., Fichefet, T., Flavoni, S., Friedlingstein, P., Grandpeix, J. Y., Guez, L., Guilyardi, E., Hauglustaine, D., Hourdin, F., Idelkadi, A., Ghattas, J., Joussaume, S., Kageyama, M., Krinner, G., Labetoulle, S., Lahellec, A., Lefebvre, M. P., Lefevre, F., Levy, C.,

Li, Z. X., Lloyd, J., Lott, F., Madec, G., Mancip, M., Marchand, M., Masson, S., Meurdesoif, Y., Mignot, J., Musat, I., Parouty, S., Polcher, J., Rio, C., Schulz, M., Swingedouw, D., Szopa, S., Talandier, C., Terray, P., Viovy, N., and Vuichard, N.: Climate change projections using the IPSL-CM5 Earth System Model: From CMIP3 to CMIP5, Clim. Dyn., 40, 2123–2165, https://doi.org/10.1007/s00382-012-1636-1, 2013.

Gent, P. R., Danabasoglu, G., Donner, L. J., Holland, M. M., Hunke, E. C., Jayne, S. R., Lawrence, D. M., Neale, R. B., Rasch, P. J., Vertenstein, M., Worley, P. H., Yang, Z.-L., and Zhang, M.: The Community Climate System Model Version 4, J. Clim., 24, 4973–4991, https://doi.org/10.1175/2011JCLI4083.1, 2011.

Harris, I., Jones, P., Osborn, T., and Lister, D.: Updated high-resolution grids of monthly climatic observations-the CRU TS3.10 Dataset, *International J. Climate.*, *34*, 623–642, https://doi.org/10.1002/joc.3711, 2014.

Heimsath, A.M., and McGlynn, R.: Quantifying periglacial erosion in the Nepal high Himalaya, *Geomorphology*, *97*, 5-23, https://doi.org/10.1016/j.geomorph.2007.02.046, 2008.

Heyman, J., Stroeven, A.P., Harbor, J.M., and Caffee, M.W.: Too young or too old: Evaluating cosmogenic exposure dating based on an analysis of compiled boulder exposure ages, *Earth. Planet. Sc. Lett.*, *302*, 71-80, https://doi.org/10.1016/j.epsl.2010.11.040, 2011.

Lee, S. Y., Seong, Y. B., Owen, L. A., Murari, M. K., Lim, H. S., Yoon, H. I. and Yoo, K.-C.: Late Quaternary glaciation in the Nun-Kun massif, northwestern India, *Boreas*, *43*, 67–89, https://doi.org/10.1111/bor.12022, 2014.

Li, Y., Li, Y., Harbor, J., Liu, G., Yi, C., and Caffee, M.W.: Cosmogenic 10Be constraints on Little Ice Age glacial advances in the eastern Tian Shan, China, *Quaternary. Sci. Rev.*, *138*, 105-118, http://dx.doi.org/10.1016/j.quascirev.2016.02.023, 2016.

Lifton, N., Sato, T., and Dunai, T.J.: Scaling in situ cosmogenic nuclide production rates using analytical approximations to atmospheric cosmic-ray fluxes, *Earth. Planet. Sc. Lett.*, *386*, 149-160, http://dx.doi.org/10.1016/j.epsl.2013.10.052, 2014.

Liu, J., Yi, C., Li, Y., Bi, W., Zhang, Q., and Hu, G.: Glacial fluctuations around the Karola Pass, eastern Lhagoi Kangri Range, since the Last Glacial Maximum, *J. Quaternary. Sci*, *32*(4), 516-527, https://doi.org/10.1002/jqs.2946, 2017.

Murari, M.K., Owen, L.A., Dortch, J.M., Caffee, M.W., Dietsch, C., Fuchs, M., Haneberg, W.C., Sharma, M.C., and Townsend-Small, A.: Timing and climatic drivers for glaciation across monsoon-influenced regions of the HimalayaneTibetan orogen, *Quaternary Science Review*, *88*, 159-182, http://dx.doi.org/10.1016/j.quascirev.2014.01.013, 2014.

Otto-Bliesner, B. L., Brady, E. C., Fasullo, J., Jahn, A., Landrum, L., Stevenson, S., Rosenbloom, N., Mai, A., and Strand, G.: Climate variability and change since 850 C.E. An ensemble approach with the Community Earth System Model (CESM), *B. Am. Meteorol. Soc.*, *97*, 735–754, https://doi.org/10.1175/BAMS-D-14-00233.1, 2016.

Owen, L.A., and Dortch, J.M.: Nature and timing of Quaternary glaciation in the Himalayan-Tibetan orogen, *Quaternary. Sci. Rev.*, *88*, 14-54, http://dx.doi.org/10.1016/j.quascirev.2013.11.016, 2014.

Owen, L.A., Robinson, R., Benn, D.I., Finkel, R.C., Davis, N.K., Yi, C., Putkonen, J., Li, D., and Murray, A.S.: Quaternary glaciation of Mount Everest, *Quaternary. Sci. Rev.*, *28*, 1412-1433, https://doi.org/10.1016/j.quascirev.2009.02.010, 2009.

Owen, L.A., Yi, C., Finkel, R.C., and Davis, N.K.: Quaternary glaciation of Gurla Mandhata (Naimon'anyi). *Quaternary. Sci. Rev.*, *29*, 1817-1830, https://doi.org/10.1016/j.quascirev.2010.03.017, 2010.

Peirce, B.: Criterion for the rejection of doubtful observations, *Astron. J.*, *2*(45), 161-163, https://doi.org/10.1086/100259, 1852.

Peng, X., Chen Y., Liu, G., Liu, B., Li, Y., Liu, Q., Han, Y., Yang, W., and Cui, Z.: Late Quaternary glaciations in the Cogarbu valley, Bhutanese Himalaya, *J. Quaternary. Sci*, *34*(1), 40-50, http://dx.doi.org/10.1002/jqs.3079, 2019.

Peng, X., Chen, Y., Li, Y., Liu, B., Liu, Q., Yang, W., Liu, G.: Late Holocene glacier fluctuations in the Bhutanese Himalaya, *Global. Planet. Change.*, *187*, 103137, https://doi.org/10.1016/j.gloplacha.2020.103137, 2020.

Ross, S.M.: Peirce's criterion for the elimination of suspect experimental data, *J. Eng. Technol-Us.*, *20*, 38-41, 2003.

Saha, S., Owen, L.A., Orr, E.N., and Caffee, M.W.: Timing and nature of Holocene glacier advances at the northwestern end of the Himalayan-Tibetan orogen, *Quaternary. Sci. Rev.*, *187*, 177-202, https://doi.org/10.1016/j.quascirev.2018.03.009, 2018.

Saha, S., Owen, L.A., Orr, E.N., and Caffee, M.W.: High-frequency Holocene glacier fluctuations in the Himalayan-Tibetan orogen, *Quaternary. Sci. Rev.*, *220*, 372-400, https://doi.org/10.1016/j.quascirev.2019.07.021, 2019.

Scherler, D., Bookhagen, B., Strecker, M.R., Blanckenburg, F., and Rood, D.: Timing and extent of late Quaternary glaciation in the western Himalaya constrained by 10Be moraine dating in Garhwal, India, *Quaternary. Sci. Rev.*, *29*, 815-831, https://doi.org/10.1016/j.quascirev.2009.11.031, 2010.

Schmidt, G. A., Kelley, M., Nazarenko, L., Ruedy, R., Russell, G. L., Aleinov, I., Bauer, M., Bauer, S. E., Bhat, M. K., Bleck, R., Canuto, V., Chen, Y., Cheng, Y., Clune, T. L., Genio, A. D., Fainchtein, R. D., Faluvegi, G., Hansen, J. E., Healy, R. J., Kiang, N. Y., Koch, D., Lacis, A., Legrande, A. N., Lerner, J., Lo, K. K., Matthews, E. E., Menon, S., Miller, R. L., Oinas, V., Oloso, A. O., Perlwitz, J. P., Puma, M. J., Putman, W. M., Rund, D., Romanou, A., Sato, M., Shindell, D. T., Sun, S., Syed, R. A., Tausnev, N., Tsigaridis, K., Unger, N., Voulgarakis, A., Yao, M.-S., and Zhang, J.: Configuration and assessment of the GISS ModelE2 contributions to the CMIP5 archive, J. Advan. in Mode. Earth Syst., 6, 141–184, https://doi.org/10.1002/2013MS000265, 2014.

Stevens, B., Giorgetta, M., Esch, M., Mauritsen, T., Crueger, T., Rast, S., Salzmann, M., Schmidt, H., Bader, J., Block, K., Brokopf, R., Fast, I., Kinne, S., Kornblueh, L., Lohmann, U., Pincus, R., Reichler, T., and Roeckner, E.: The atmospheric component of the MPI-M earth system model: ECHAM6, J. Adv. Model. Earth Syst., 5, 1–27, https://doi.org/10.1002/jame.20015, 2013.

Wu, T., Song, L., Li, W., Wang, Z., Zhang, H., Xin, X., Zhang, Y., Zhang, L., Li, J., Wu, F., Liu, Y., Zhang, F., Shi, X., Chu, M., Zhang, J., Fang, Y., Wang, F., Lu, Y., Liu, X., Wei, M., Liu, Q., Zhou, W., Dong, M., Zhao, Q., Ji, J., Li, L., and Zhou, M.: An overview of BCC climate system model development and ap plication for climate change studies, J. Met. Res., 28, 34–56, https://doi.org/10.1007/s13351-014-3041-7, 2014.

Yang, W., Han, Y., Peng, X., Ran, Z., Liu, Q., and Liu, G.: Paleoglacial and paleoclimate reconstructions during the global Last Glacial Maximum in the Longriba area, eastern Tibetan Plateau, *Journal of Mountain Science*, *18*(2), 307-322, https://doi.org/10.1007/s11629-020-6238-5, 2021.

Zech, R., Zech, M., Kubik, P.W., Kharki, K., and Zech, W.: Deglaciation and landscape history around Annapurna, Nepal, based on 10Be surface exposure dating, *Quaternary. Sci. Rev.*, *28*, 1106-1118, http://doi.org/10.1016/j.quascirev.2008.11.013, 2009.

Zhang, Q., Yi, C., Dong, G., Fu, P., Wang, N., and Capolongo, D.: Quaternary glaciations in the Lopu Kangri area, central Gangdise Mountains, southern Tibetan Plateau, *Quaternary. Sci. Rev.*, *201*, 470-482, https://doi.org/10.1016/j.quascirev.2018.10.027, 2018.